Science of The Total Environment
April 2024, Volume 922 Pages 171385 (14p.)
https://doi.org/10.1016/j.scitotenv.2024.171385
https://archimer.ifremer.fr/doc/00880/99178/

Distribution of rare earth elements and assessment of anthropogenic gadolinium in estuarine habitats: The case of Loire and Seine estuaries in France

Rétif Julie [1, *], Briant Nicolas [2], Zalouk-Vergnoux Aurore [1], Le Monier Pauline [2], Sireau Teddy [2], Poirier Laurence [1]

[1] Nantes Université, Institut des Substances et Organismes de la Mer, ISOMer, UR 2160, F-44000 Nantes, France
[2] Ifremer, CCEM Contamination Chimique des Écosystèmes Marins, F-44000 Nantes, France

* Corresponding author : Julie Rétif, email address : julie.retif@univ-nantes.fr

Nicolas.Briant@ifremer.fr ; aurore.zalouk-vergnoux@univ-nantes.fr ; Pauline.Le.Monier@ifremer.fr ; Teddy.Sireau@ifremer.fr ; laurence.poirier@univ-nantes.fr

Abstract :

Rare earth elements (REEs), attractive to society because of their applications in industry, agriculture and medicine, are increasingly released into the environment especially in industrialized estuaries. This study compared the REE distribution in the abiotic compartments: water (dissolved phase (<0.45 µm), suspended particulate matter (SPM)) and sediment of the Loire and Seine estuaries (France). A total of 8 and 6 sites were investigated in the Loire and Seine, respectively, as well as 5 additional offshore sites for the Loire. Total REE concentrations were higher in the Loire for the dissolved phase (93.5 ± 63.3 vs 87.7 ± 16.2 ng/L), SPM (173.9 ± 18.3 vs 114.0 ± 17.8 mg/kg dw) and sediments (198.2 ± 27.9 vs 73.2 ± 27.4 mg/kg dw), explained by higher geogenic inputs. Individual REE contributions along with normalization highlighted heavy REE enrichments and Gd positive anomalies in the dissolved phase of the two estuaries, whereas REE distributions in SPM and sediments followed the natural abundance of the REE classes. The calculated Gd anomalies in the dissolved phase were higher in the Seine (9.7 ± 3.4) than in the Loire (3.0 ± 0.8), corresponding to 88.3 ± 5.1 % and 64.4 ± 11.1 % of anthropogenic Gd. This demonstrates a higher contamination of the Seine estuary, certainly due to the difference in the number of inhabitants between both areas involving different amounts of Gd used in medicine. Offshore sites of the Loire showed lower total REE concentrations (55.8 ± 5.8 ng/L, 26.7 ± 38.2 mg/kg dw and 100.1 ± 11.7 mg/kg dw for the dissolved phase, SPM and sediments, respectively) and lower Gd anomalies (1.2 ± 0.2) corresponding to only 13.3 ± 3.9 % of anthropogenic Gd, confirming a contamination from the watershed. This study comparing two major French estuaries provides new data on the REE distribution in natural aquatic systems.

Graphical abstract

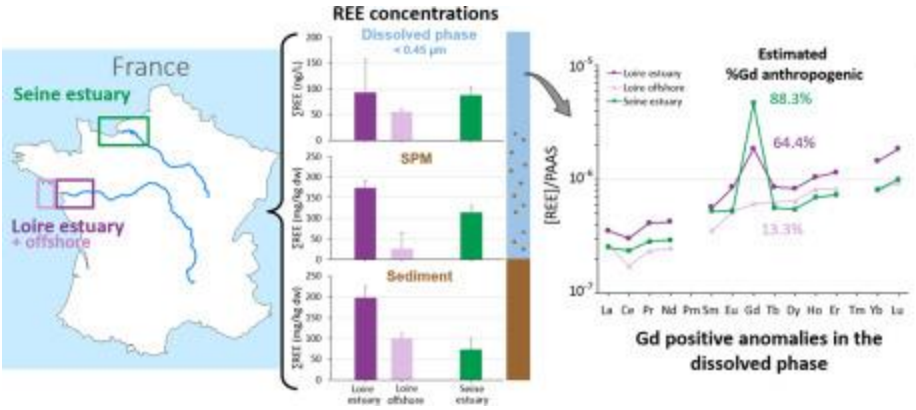

Highlights

► Total REE concentrations were higher in the Loire estuary than in the Seine estuary. ► Gd positive anomalies were reported in the dissolved phase of the two estuaries. ► The Gd anthropogenic contamination was higher in the Seine than in the Loire. ► REE concentrations and Gd anomalies were lower offshore than in the estuary of Loire. ► First study about the REE concentration and distribution in the Seine estuary.

Keywords : Gd anomaly, abiotic compartments, dissolved phase, suspended particulate matter, sediment

1. Introduction

Estuaries are unique dynamic physical and ecological systems at the interface between marine and freshwater environments. They constitute very rich particular ecosystems including wetlands, mudflats, (salt) marshes, valleys, forests, woods, bocages or (wet) meadows, very rich faunistically and floristically, promoting biodiversity. They also play a crucial role as habitat (nursery, feeding or migratory areas) for many aquatic and bird species. However, these areas, being really attractive economically because of their natural richness, are subject to strong anthropogenic pressure due to the high population density and the associated human activities and industrialization along their banks. These activities induce a discharge of contaminants, especially trace metals, into the environment reaching then estuaries. Acting as transition zones between the continent and the oceans, estuarine areas, are therefore particularly sensitive to contaminants as they are the receptable of both

anthropogenic and natural inputs from large watersheds. Moreover, estuaries are constantly changing environments subject to significant variations in salinity, turbidity and water level, coupled with daily and seasonal variations, such as tides, river flow and temperature, all influencing the fate of contaminants in these complex and dynamic environments.

Among trace metals, rare earth elements (REEs) attract more and more interest due to their remarkable electromagnetic, optical and catalytic properties. They are widely used in industry as permanent magnets, catalysts, phosphors, in new technology devices (laptops, optic fibers etc.), in renewable energy (such as wind turbines or solar panels) (Castor & Hedrick, 2006; Bru et al., 2015; Zhou & Fiete, 2020) and also in agriculture and aquaculture (Ozaki et al., 2000; Abdelnour et al., 2019). Another increasing use of REEs is in medicine, where chelate forms of Gd are extensively used as contrast agents for MRI (magnetic resonance imaging; Blomqvist et al., 2022) which results in significant releases of Gd into the environment through the releases of wastewater treatment plants (WWTP), as demonstrated by many studies (Kümmerer & Helmers, 2000; Rabiet et al., 2009; Verplanck et al., 2010; Rogowska et al., 2018; Laczovics et al., 2023).

REEs gather the fifteen lanthanoids (lanthanum (La), cerium (Ce), praseodymium (Pr), neodymium (Nd), promethium (Pm), samarium (Sm), europium (Eu), gadolinium (Gd), terbium (Tb), dysprosium (Dy), holmium (Ho), erbium (Er), thulium (Tm), ytterbium (Yb) and lutetium (Lu)) as well as scandium (Sc) and yttrium (Y). They are regrouped into three classes on the basis of their molecular weight (Bru et al., 2015): the light REEs (LREEs: La to Pm), the medium REEs (MREEs: Sm to Gd) and the heavy REEs (HREEs: Tb to Lu). All REEs, share similar chemical properties provided by their comparable electronic configuration: partially filled 4f electron shell, providing previously described unique electromagnetic properties.

The release of these elements into the environment causes a progressive enrichment in aquatic ecosystems which can disturb their natural abundance and biogeochemical cycle. Indeed, REEs are naturally present in the Earth's crust and are mostly found in the trivalent oxidation level (III) in the environment. Nevertheless, some of them, such as Ce and Eu, can be oxidized or reduced to Ce (VI) and Eu (II) under certain conditions (de Baar et al., 1985a). REE's behavior in aquatic ecosystems is well documented and showed their solubility can be influenced by several physicochemical

parameters, such as salinity, pH or suspended particulate matter (SPM) quantity (Elderfield & Greaves, 1982; Sholkovitz & Szymczak, 2000; Tepe & Bau, 2016; Thibault de Chanvalon et al., 2016). In aquatic systems, REEs are mostly accumulated in the sediment than in the dissolved phase of the water column, as they tend to coagulate in colloids and to aggregate with SPM to end up in sediment (Tepe & Bau, 2016; Thibault de Chanvalon et al., 2016). Total REE concentrations reported in estuarine sediments are in the order of magnitude of mg/kg (Borrego et al., 2004; Marmolejo-Rodríguez et al., 2007; Brito et al., 2018; Chi et al., 2021; de Freitas et al., 2021; Santos et al., 2023) while it is much lower in the dissolved phase of the water column (ng/L; Kulaksiz & Bau, 2013; Tepe & Bau, 2016; Cánovas et al., 2020) but with more reported anomalies (Elbaz-Poulichet et al., 2002; Censi et al., 2007; da Costa et al., 2021). REE enrichments, such as La, Sm, Gd or Tb, have already been highlighted in different studies on freshwater (Elbaz-Poulichet et al., 2002; Kulaksiz & Bau, 2013; Merschel & Bau, 2015) and marine ecosystems (de Baar et al., 1985b; Alibo & Nozaki, 1999; da Costa et al., 2021), possibly due to their anthropogenic use in industrial, agricultural or medical fields. In addition, studies investigating Gd showed an increase in the recorded anomaly values highlighting a Gd enrichment over time (Hatje et al., 2016; Lerat-Hardy et al., 2019), probably linked to its use in medicine.

The increase of REE concentrations in the environment, their possible bioaccumulation within aquatic organisms (Li et al., 2016; Wang et al., 2019; Briant et al., 2021; Rétif et al., 2024) and their potential toxic effects (Perrat et al., 2017; Cardon et al., 2019; Freitas et al., 2020) demonstrate the importance of investigating their distribution in natural environments, such as estuaries. The analysis of all abiotic compartments is necessary to better characterize the contamination of ecosystems by REEs as well as their fate and their bioavailability to organisms. However, most studies have not investigated all the abiotic compartments, focusing on either the sediment (Borrego et al., 2004; Brito et al., 2018; Costa et al., 2021) or the water column (Adebayo et al., 2020; Cánovas et al., 2020). Another essential goal is to understand the role of estuarine environments in the dynamics of REEs at the land-ocean interface. Similar to other pollutants, the challenge lies on determining whether estuaries act as sinks, sources or modifiers of REE behavior. However, there is a lack of research on the REE behavior in French estuaries, especially in the Seine estuary while the Loire (Thibault de

Chanvalon et al., 2016; Lortholarie, 2021) and the Gironde (Lerat-Hardy et al., 2019) estuaries have already been studied.

The Loire and Seine estuaries share several similarities suggesting that their environmental and ecological characteristics may exhibit comparable dynamics and behaviors. They are both defined as macrotidal linked to their tidal ranges up to 6 m (Boët et al., 2011). They have variable extension of the maximum turbidity zone (MTZ) according to water flows and tidal ranges (GIP, 2014). The variability of the annual mean particulate organic carbon (POC) content in the Seine estuary was found to be similar to that in the Loire estuary (Etcheber et al., 2007). Furthermore, fish composition and assemblage structure indicate similarities between these estuaries (Selleslagh et al., 2009). This study, therefore aims to evaluate and compare the REE abiotic concentrations and possible anthropogenic contamination of the Loire and Seine estuaries. Total REE concentrations, as well as individual REE contributions, were measured in the abiotic compartments (dissolved phase and SPM of the water column; sediment) of several sites from both estuaries. The Post Archean Australian Shale (PAAS) normalization was used to account for geogenic inputs and to estimate anthropogenic inputs. Finally, Gd anomalies and anthropogenic Gd concentrations were calculated for the dissolved phase and compared between the two estuaries.

2. Material and methods

2.1. Study areas

The two studied areas, the Loire estuary and the Seine estuary, have different topographies and levels of pollution (Romana, 1994). The Loire estuary is 97 km long, from Ancenis to Saint Nazaire. The water reaching this estuary drains the largest watershed in France (118,000 km²; GIP Loire-Estuaire, Agence de l'Eau Loire-Bretagne) covering 20 % of the total French territory and gathering about 13 million inhabitants. The estuarine area is highly industrialized and has a large agriculture activity as well as a high population density, mainly concentrated in the Nantes metropolis (about 650,000 inhabitants) and the city of Saint Nazaire (about 70,000 inhabitants).

The Seine estuary extends for 160 km, from Poses to Le Havre and drains a smaller watershed of 79 000 km² (GIP Seine-Aval, Agence de l'Eau Seine-Normandie), but gathers 30 % of the total French

population (about 18 million inhabitants), including the Paris metropolis. The Seine basin accounts for 50 % of the national river transport, as well as 40 % of the national economic activity (including agricultural and industrial activities), making it the most developed and industrialized river network in France (Romana, 1994; Lafite & Romana, 2001). The estuarine area is under strong anthropogenic pressure mainly from two cities: the Rouen metropolis (about 490,000 inhabitants) and the city of Le Havre (160,000 inhabitants).

In 2013, the patterns of land use and water management (SAGE: Schéma d'Aménagement et de Gestion des Eaux) reports on the chemical water quality of the Loire and Seine estuaries, carried out by Agence de l'Eau Loire-Bretagne and Agence de l'Eau Seine-Normandie, respectively, stated to a – bad – chemical status for both estuaries. They were reconducted in 2017 and 2019 for the Loire estuary and the Seine estuary, respectively, and led to the same result. The REE levels of the Loire estuary have already been investigated (Thibault de Chanvalon et al., 2016; Lortholarie, 2021), but to our knowledge, no investigation of the Seine estuary for REE contamination has been performed so far.

2.2. Sampling

The sampling of the two estuaries were carried out one year apart but during the same season to limit seasonal variations: in April 2021 for the Loire estuary and in April 2022 for the Seine estuary. In the Loire, 13 sites were sampled including 8 estuarine sites: Ancenis (L1), Bellevue (L2), Rezé (L3), Haute Indre (L4), Cordemais (L5), Paimboeuf (L6), Donges (L7) and Mindin (L8) and 5 offshore sites: L9, L10, L11, L12 and L13. In the Seine, 6 estuarine sites were sampled: Poses (S1), Duclair (S2), Caudebec (S3), Vieux port (S4), Tancarville (S5) and Baie de Seine (S6) (**Table S1**, **Figure 1**). The estuarine sites of the two estuaries are impacted by different anthropogenic REE sources related to their two main uses in industry (as permanent magnets, in oil catalytic cracking or metallurgical alloys) and in medicine (especially nuclear medicine for MRI). In the Loire estuary, there are several WWTP: near Ancenis, Nantes and Mindin, as well as an aeronautical industry in Nantes, a coal-fired power plant in Cordemais, a refinery in Donges (the second largest in France) and the harbor shipyard of Saint Nazaire. The Seine estuary regroups three refineries including the first

and the third largest in France near Le Havre (Gonfreville-l'Orcher) and Tancarville (Port-Jérôme-sur-Seine), respectively, as well as one near Rouen (Petit-Couronne). In addition to the coal-fired power plant and the industrial harbor of Le Havre, there are also many WWTP: near Poses, Rouen, Duclair, Caudebec, Tancarville and Le Havre. The Loire offshore sites are considered to be less exposed to anthropogenic inputs due to their location further from the watershed.

Samples of surface water and intertidal sediments were collected at the 8 estuarine sites of Loire (L1 to L8) and the 6 estuarine sites of Seine (S1 to S6) (**Table S1**, **Figure 1**). At each site, three surface (< 10 cm depth) sediment samples (500 g) were collected, at low tide using an acid-cleaned plastic sampling cup, in clean plastic bags, on three 50 cm length squares, randomly selected but distanced by at least 1.5 m apart. Then, 2 L of water were collected with a sampling cane in prewashed (HNO_3 10 %) plastic bottles. In addition, for the sites L5, L7 and L8 of Loire, subtidal sediments (1 to 15 m depth) were collected in clean plastic bags using an Ekman grab from a boat. Following the same methodology, surface water and subtidal sediments (20 to 23 m depth) were collected at the 5 offshore sites of Loire (L9 to L13), except for L9 and L11 where only subtidal sediments and surface water were sampled, respectively (**Table S1**, **Figure 1**).

Physicochemical parameters (including: temperature (T, °C), dissolved oxygen (DO, mg/L), salinity (S, g/L), conductivity (C, mS/cm), suspended particulate matter (SPM, g/L) and mean daily water discharge (Q, m^3/s)) were recorded either directly in the field (for temperature), back in the laboratory (for salinity and SPM) or thanks to the SYVEL and SYNAPSES networks, from GIP Loire Estuaire and GIP Seine-Aval, respectively (**Table S1**). The mean daily water discharges during the sampling periods were of 503 to 807 m^3/s and 320 to 342 m^3/s for the Loire and Seine, respectively.

2.3. Sediment characterization

After collection, intertidal and subtidal sediments were aliquoted for grain size analysis and stored at 4 °C. Sediment grain size was determined for each site by laser diffraction using a laser granulometer (Malvern Mastersizer 3000) with a hydro-module (MV). About 0.1 g of fresh sediment

was weighted and mixed with 100 mL of demineralized water under magnetic stirring for 15 min. The samples were then introduced into the granulometer at a rotation of 1000 rpm. After reaching sufficient obscuration, 3 measures were taken per sample. Gradistat software was used allowing to determine the volume average particle size in µm (D_{50}) as well as D_{10} and D_{90}.

The rest of sediment samples were frozen (-20 °C), freeze-dried, ground, homogenized and sieved at 2.5 mm. The organic matter (OM) content of sediment samples was estimated from the dried sediments. About 5 g were weighed in aluminum cups and calcined in a muffle furnace (Nabertherm LE) at 550 °C for 5 h. The ashes from the calcination were weighed and the difference in weight was used to estimate the OM content (%).

2.4. Sample preparation for ICP-MS analysis

2.4.1. Sediments

Sample preparation was performed on freeze-dried sediments. Briefly, 200 mg of dry sediments were digested with a mixture of 250 µL of HNO_3, 750 µL of HCl and 6 mL of HF, in a tube placed on a hot plate at 130 °C during four hours, before being evaporated to dryness at 100 °C. A second, 6-hour digestion step was performed at 130 °C with a mixture of 4 mL of HNO_3 and 20 mL of high purity water. The acid digests were then transferred to Falcon® tubes and brought to a final volume of 50 mL with ultrapure water. Three procedural blanks and international certified reference materials (BCR-667, estuarine sediment and PACS-3, marine sediment, NRC, Canada) were also processed with the samples.

2.4.2. Water

Suspended particle matter

Cellulose nitrate filters (0.45 µm) were pre-weighed in acid-washed Petri dish and dried out at 60 °C before use. A volume of 1 L of water per site was filtered using the prepared filters to separate SPM from the dissolved phase. After water filtration, the filters were dried at 60 °C for 24 hours,

weighed and stored at -20 °C. Finally, they were digested following the same protocol than for sediments, including the processing of procedural blanks and certified reference materials.

Dissolved phase

Filtered water samples were acidified to 0.2 % v/v HNO_3 and stored at 4 °C prior to preparation based on the study of Hatje et al. (2014). Briefly, at the Ifremer's cleanroom, the samples were preconcentrated and separated from the saline matrix using columns filled with Nobias Chelate PA1 resin (Hitachi High Technologies®). Then, 100 to 150 mL of each sample, spiked with Tm (50 ng/L) and adjusted at pH 4.7 ± 0.02 with buffer solution (NH_4Ac 2.5 M), were loaded onto the columns at a speed of 1 mL/min using a peristaltic pump (ISMATEC). The columns were then rinsed with 5 mL of NH_4Ac 0.05 M, and REEs were eluted with 1 mL of HNO_3 1 M. To control the quality of the preconcentration, blanks consisting of "clean" seawater (free of trace metals), reference material (CASS-6, seawater, NRC, Canada) and spiked seawater (10 ng/L of REEs), were processed on each series.

2.5. Rare earth elements and Aluminum analysis by ICP-MS

REE analysis of the abiotic compartments was performed using a TQ-ICP-MS (iCAP-TQ Thermo®) in KED mode with He as collision gas. Selected REE isotopes were the following: ^{139}La, ^{140}Ce, ^{141}Pr, ^{144}Nd, ^{146}Nd, ^{147}Sm, ^{149}Sm, ^{153}Eu, ^{157}Gd, ^{159}Tb, ^{163}Dy, ^{165}Ho, ^{166}Er, ^{169}Tm, ^{172}Yb and ^{175}Lu. Aluminum (^{27}Al) was also analyzed in sediment and SPM samples. External calibration using multi-element standard solutions (SCP Science) was performed at the beginning of each analytical session. Indium (^{115}In, 2 ppb) was used as an internal standard in each sample. As quality controls, instrument blanks (6 % HNO_3) and standard solutions containing 0.1 µg/L of REE were running on the ICP-MS every 10 samples. The REE concentrations in the blanks were subtracted from the sample concentrations. The limits of detection (LOD) and of quantification (LOQ) were determined in ng/L and mg/kg dw for each REE as follows: LOD = (mean of blanks + 3 * standard deviation of blanks) and LOQ = (mean of blanks + 10 * standard deviation of blanks) (**Table S2**).

2.6. REE normalization and anomalies calculation

REE concentrations are reported in nanograms per liter (ng/L) for the dissolved phase and in milligrams per kilogram of dry weight (mg/kg dw) for SPM and sediments. Total REE concentrations (ΣREE) were calculated as the sum of the individual REEs, and individual REE contributions were calculated as the mean percentage (%) for each REE. The mean values ± standard deviations (SD) were used to describe the data. The LREEs included La to Nd, the MREEs: Sm to Gd and the HREEs: Tb to Lu. Pm was excluded because it is radioactive and not naturally present in the environment.

To visualize anomalies, REE concentrations were normalized to Post Archean Australian Shale (PAAS; Pourmand et al., 2012; Rétif et al., 2023). The geogenic background concentration of Gd was estimated by modeling the shape of the normalized REE pattern using a third-order polynomial fit (Möller et al., 2002, 2003; Hatje et al., 2016) excluding Ce and Eu due to their redox sensitivity as well as Gd because it is often anomalous. Gd anomalies were then calculated using the **equation (1)**:

$$\text{eq (1):}\quad Gd_N / Gd_N^* = Gd_N / (ax^3 + bx^2 + cx + d)$$

where Gd_N is the PAAS-normalized Gd concentration and Gd_N^* is the geogenic background Gd concentration calculated by solving each fitted third-order polynomial of a, b, c and d parameters for x = 8 (Gd position) (da Costa et al., 2021). Values higher than 1 indicate positive anomalies and values lower than 1 indicate negative anomalies.

Finally, the anthropogenic Gd concentrations (Gd_{anth}) were calculated using the **equation (2)** (Hatje et al., 2016). Their percentage was then calculated, allowing the contribution of anthropogenic inputs to the total measured Gd concentration to be estimated.

$$\text{eq. (2):}\quad Gd_{anth} = Gd_N - Gd_N^*$$

2.7. Statistical analysis

Statistical analysis was carried out using Rstudio. ANOVA tests were used for multiple group comparisons. First, Levene's tests were performed on the raw data to verify the homogeneity of the

variances. The normality of the data was then checked by using a Shapiro-Wilk test. If the results of these first two tests were positive, the ANOVA was carried out on the raw data, otherwise values were either log10- or sqrt-transformed to improve the data normality. Finally, if the ANOVA result indicated significant differences between the studied groups, they were identified by performing a Tukey's HSD post-hoc multiple comparison test. For two-group comparisons, t-student tests were performed after verifying the data distribution normality and the variance homogeneity with a Shapiro-Wilk test and a Bartlett's test, respectively. Since the anomaly data did not meet the normality requirement, Kruskal-Wallis tests were used followed by post-hoc Nemenyi tests for multiple comparisons. Finally, Wilcoxon's tests were performed to verify the presence of anomalies (values $\neq 1$). The significance level for all statistical tests was set at $p\text{-}value \leq 0.05$.

3. Results

3.1. REE concentrations

Total REE concentrations for the studied abiotic compartments are shown in **Figure 2**. REE concentrations were the lowest in the dissolved phase for both estuaries. However, the results between SPM and sediments differed between the two estuaries, *i.e.* REE levels were the highest in sediment for the Loire estuary whereas they were the highest in SPM for the Seine estuary.

Regarding the dissolved phase (**Figure 2A, B**, **Table S3**), the REE concentrations reported in estuarine sites (L1 to L8 and S1 to S6) of both estuaries were relatively similar but slightly higher in the Seine estuary (73.1 to 116.3 ng/L for S3 and S4, respectively) than in the Loire estuary (45.1 to 234.5 ng/L for L7 and L8, respectively). No significant differences were observed between the studied sites, except in the Loire with much higher REE levels in L8 corresponding to Mindin (234.5 ng/L). The other sites in the Loire estuary had a mean value of 73.4 ± 29.7 ng/L with generally higher values in upstream sites (L1 to L4, 65.5 – 113.9 ng/L) than downstream sites (L5 to L7, 45.1 – 46.4 ng/L). In the Seine, REE levels were more homogenous among the different sites investigated. Moreover, the concentrations reported in the offshore sites of Loire (L9 to L13, 48.4 – 62.2 ng/L) were generally in the same range than those recorded in the estuary (L1 to L8).

Concerning SPM (**Figure 2C, D**, **Table S4**), REE concentrations were higher in the Loire estuary (130.4 ± 13.2 to 186.4 mg/kg dw for L8 and L4, respectively) than in the Seine estuary (97.0 ± 10.9 to 141.9 ± 4.88 mg/kg dw for S6 and S5, respectively). The reported concentrations in the estuarine sites of each estuary (L1 to L8 and S1 to S6) were quite homogenous with only significant differences between sites L6 and L8 for the Loire estuary and between sites S5 and S6 for the Seine estuary. However, conversely to the dissolved phase, the offshore sites (L9 to L13) diverged from the estuarine sites (L1 to L8) of Loire with much lower REE levels (3.37 to 83.5 mg/kg dw for L12 and L10, respectively).

The results for sediments (**Figure 2E, F**, **Table S5**) were similar to those of SPM. REE concentrations of intertidal samples from estuarine sites (L1 to L8 and S1 to S6) were higher in the Loire (125.6 ± 40.8 to 221.7 ± 64.1 mg/kg dw for L1 and L8, respectively) than in the Seine (20.0 ± 4.39 to 97.8 ± 3.71 mg/kg dw for S2 and S6, respectively). In the Loire estuary, no difference in REE levels was observed between intertidal and subtidal samples (L5: 210.5 ± 17.4 *vs* 225.6 ± 43.6 mg/kg dw; L7: 182.3 ± 8.01 *vs* 203.1 ± 11.5 mg/kg dw; L8: 221.7 ± 64.1 *vs* 221.3 ± 25.8 mg/kg dw). In the Seine estuary, the site S2 stood out from the others with the lowest concentrations (20.0 ± 4.4 *vs* 83.9 ± 9.5 mg/kg dw in average for the other sites). Similarly to SPM, the REE levels recorded in the Loire offshore sites (L9 to L13, 85.8 ± 14.6 to 114.5 ± 15.4 mg/kg dw) were significantly lower than those reported in the estuary (L1 to L8).

3.2. REE distribution

The individual REE contributions in the abiotic compartments of the two estuaries were investigated (**Figure 3**) and showed similar distribution patterns from SPM and sediment samples (LREEs >> MREEs ≥ HREEs) in contrast to those from the dissolved phase (LREEs ≥ MREEs > HREEs). Indeed, the dissolved phase patterns of both estuaries showed much higher percentages of MREEs (especially Gd) and HREEs, compared to those of SPM and sediments, with globally lower associated LREE percentages.

The results of the REE distribution in the dissolved phase of both estuaries are presented in **Figure 3A, B** and **Table S6**. Regarding estuarine sites (L1 to L8 and S1 to S6), both estuaries showed a higher contribution of LREEs (with a Ce predominance) compared to MREEs and HREEs with 50.1 to 79.2 % in the Loire and 40.3 to 63.0 % in the Seine. The highest difference between the two estuaries was in the MREE contribution, reaching 10.7 to 25.8 % and 24.6 to 49.4 % for the Loire and Seine, respectively. These high values of MREEs were mainly due to the Gd contribution which was greater in the Seine (19.0 – 44.4 %) than in the Loire (6.3 – 20.2 %) estuarine sites and explained the variation of the MREE contribution between the two estuaries. HREEs showed the lowest contribution for both estuaries with a higher percentage in the Loire (10.0 to 23.6 %) than in the Seine (9.0 to 12.4 %). The lower contribution of LREEs and HREEs recorded in the Seine compared to the Loire was probably due to the higher Gd contribution reported in the Seine estuary. Concerning the spatial comparison of the estuarine sites of each estuary, variations (especially for the Gd contribution) were noticeable. Concerning the Loire estuary, they were mostly visible for the site L8, having a much lower contribution of Gd (6.3 *vs* 16.0 ± 4.1 % in the other Loire estuarine sites) and MREEs (10.7 *vs* 21.6 ± 3.9 %), thus increasing the LREE contribution (79.2 *vs* 58.6 ± 7.1 %) and explaining its diverging distribution pattern. In the Seine estuary, the Gd contribution was the lowest at site S6 and highest at site S3. Finally, the offshore sites (L9 to L13) diverged from the estuarine sites (L1 to L8) of Loire with a much lower Gd contribution (6.5 – 6.8 %), decreasing the global MREE contribution (12.0 – 12.4 %) and increasing the LREE contribution, reaching 68.6 to 70.7 %. However, the HREE contribution was similar between offshore and estuarine sites (17.4 to 19.1 % and 10.0 to 23.6 %, respectively). Thus, the REE distribution patterns for offshore sites, as well as L8 site were close to the patterns of SPM and sediments and showed the following distribution order: LREEs > HREEs > MREEs.

Regarding the SPM REE distribution patterns (**Figure 3C, D**, **Table S7**) of both estuaries, they were similar with a contribution of LREEs of 86.4 ± 0.2 % and 85.6 ± 0.3 %, MREEs of 7.5 ± 0.1 % and 7.4 ± 0.2 % and HREEs of 6.1 ± 0.2 % and 7.0 ± 0.1 %; in the estuarine sites of Loire (L1 to L8) and Seine (S1 to S6), respectively. The predominant REE for each class were the same in both

estuaries, *i.e.* Ce for LREEs, Sm for MREEs and Dy for HREEs. Concerning the site comparison, no differences were highlighted either between estuarine sites of the two estuaries or between the estuarine (L1 to L8) and offshore (L9 to L13) sites of Loire, since the percentages of offshore sites were comparable with 87.4 ± 2.6 %, 6.9 ± 0.6 % and 5.7 ± 2.1 % for LREEs, MREEs and HREEs, respectively. Only L10 slightly differed from the other studied sites with a lower HREE contribution of 3.1 % (*vs* 6.3 ± 0.6 % in all the other sites of Loire) resulting in a higher contribution of LREEs (90.1 *vs* 86.4 ± 0.7 %).

Comparably to SPM, the sediment distribution patterns were relatively similar between the two studied estuaries (**Figure 3E, F**, **Table S8**). The LREE and MREE percentages of intertidal estuarine sites (L1 to L8 and S1 to S6) were quite close with 86.8 ± 0.2 % and 83.2 ± 1.0 % of LREEs, 7.3 ± 0.1% and 8.2 ± 0.3 % of MREEs in the Loire and Seine, respectively. The HREE percentages differed though with a higher percentage in the Seine estuary (8.5 ± 0.8 %) compared to the Loire estuary (5.9 ± 0.2 %), resulting in a divergent distribution pattern in the sediments of Seine (LREEs > HREEs ≥ MREEs). The two estuaries had a predominance of Ce, Sm and Dy in LREEs, MREEs and HREEs, respectively. As for the results of REE concentrations, no differences of REE contribution were highlighted between intertidal and subtidal sediments from the Loire sites combining these two types of sampling. Similarly to SPM, no differences were found between estuarine sites of both estuaries nor between the estuarine (L1 to L8) and offshore (L9 to L13) sites of Loire. The average contributions of offshore sites were of 88.4 ± 0.6 %, 7.0 ± 0.3% and 4.6 ± 0.3 % for LREEs, MREEs and HREEs, respectively.

3.3. Gd anomalies and anthropogenic concentrations

REE concentrations normalized to PAAS are presented in **Figure 4**. The patterns of the dissolved phase (**Figure 4A, B**) of waters from the two estuaries showed MREE and HREE enrichments compared to LREEs with negative Ce anomalies and positive Eu and Gd anomalies. The Ce and Eu anomalies were lower in the Seine than in the Loire. Conversely, the Gd anomalies were of higher magnitude in the Seine than in the Loire and in the estuarine sites (L1 to L8) compared to the offshore

sites (L9 to L13) of Loire. Regarding SPM (**Figure 4C, D**) and sediments (**Figure 4E, F**), the REE patterns of both estuaries were similar with a HREE depletion, more visible in the Loire estuary than in the Seine estuary for both matrices as well as different Eu anomalies (positive or negative) especially noticeable in the Loire. Similarly to the REE distributions, there were no differences between normalized REE patterns from intertidal and subtidal sediments, as well as from the estuarine and offshore sites of Loire.

Ce, Eu and Gd anomalies were calculated and are presented for the dissolved phase in **Figure 5** and **Table S3**. The values were presented according to the estuary. Ce anomalies were negative and significantly higher in the Seine estuary (0.87 ± 0.04) compared to the Loire estuary, where anomalies were lower in estuarine sites (0.72 ± 0.14) compared to offshore sites (0.76 ± 0.04) (**Figure 5A**). The same trend was observed for the Eu anomalies with significantly higher values in the estuarine sites (1.36 ± 0.07) compared to the offshore sites (1.17 ± 0.05) of Loire and to the Seine estuary (1.14 ± 0.05) (**Figure 5B**). The highest differences were observed for the Gd anomalies. The Seine estuary values were significantly higher (mean value of 9.70 ± 3.40) compared to the Loire, with higher values in estuarine sites (3.02 ± 0.80) than in offshore sites (1.16 ± 0.05) (**Figure 5C**). Gd anomalies in estuarine sites ranged from 4.71 to 14.66 for S6 and S3 in the Seine and from 1.73 to 3.90 for L8 and L2 in the Loire. These results are consistent with the normalization patterns reported in the dissolved phase of both estuaries (**Figure 4**) showing a higher magnitude of Gd anomalies in the Seine than in the Loire and in estuarine sites compared to offshore sites.

Anthropogenic Gd concentrations were estimated based on the calculation of geogenic Gd concentrations. Their contributions to the total measured Gd concentrations in the dissolved phase of each site of the two estuaries are presented in **Figure 6** and **Table S3**. Both estuaries showed Gd anthropogenic inputs but they were much greater in the Seine estuary (S1 to S6), corresponding to 78.8 to 93.2 % of the total measured Gd, compared to the estuarine sites of Loire (L1 to L8) reaching 42.2 to 74.3 %. Inter-site variations were also noticeable. In the Loire, L8 showed the highest total Gd concentration, mainly due to geogenic Gd (57.8 % of the total measured Gd *vs* 32.5 ± 7.1 % for the other estuarine sites of Loire) also corresponding to the site with the lowest anthropogenic

contribution. The highest anthropogenic Gd contribution was measured in L2 (**Figure 6A**). In the Seine, S4 showed the highest total and anthropogenic Gd concentrations. The highest and lowest anthropogenic Gd contributions were recorded in S3 and S6, respectively (**Figure 6B**). Finally, the anthropogenic Gd contribution in the offshore sites (L9 to L13) of Loire was much lower than in the estuary (L1 to L8), reaching only 9.5 to 18.6 % (**Figure 6A**).

4. Discussion

4.1. REE concentrations

Overall, the REE concentrations measured in the abiotic compartments of both estuaries are comparable to many other studies focusing on REEs in abiotic compartments (**Table 1**). Regarding the dissolved phase, the range of REE concentrations measured in this study (45.1 – 234.5 ng/L in the Loire and 73.1 – 116.3 ng/L in the Seine, **Table S3**) was similar to those reported in the water of the Huelva estuary in Spain (26 to 380 ng/L; Cánovas et al., 2020) and of the Gironde estuary in France (93.9 – 182.5 ng/L; Lerat-Hardy et al., 2019). They were mostly lower than those recorded in river and estuarine waters from Europe and USA, as well as in Pacific and Atlantic seawater (22 to 2,134 ng/L; Kulaksiz & Bau, 2013; Tepe & Bau, 2016; Adebayo et al., 2020). The recorded values are also lower than those previously measured in the Loire estuary (234 to 1,140 ng/L; Lortholarie, 2021), possibly due to flow variations between the different sampling periods. Indeed, the sampling of the present study was performed in April as opposed to December in the Lortholarie study (2021), involving possible high variations in the daily water discharge of the Loire estuary, influenced by seasonal parameters and therefore impacting the measured REE concentrations. The reported REE values in SPM of different estuaries and rivers from China, India, Thailand and Brazil (2.8 to 534.4 mg/kg dw; Censi et al., 2007; Chunye et al., 2008; Shynu et al., 2011; Han et al., 2021, 2023; Santos et al., 2023) were in the same range as those measured in the Loire (3.4 – 186.4 mg/kg dw) and Seine (97.0 – 141.9 mg/kg dw) estuaries (**Table S4**). The investigation of estuarine sediments from Spain, Thailand, Mexico, India, China, Portugal and Brazil revealed REE concentrations from 14.2 to 253.3 mg/kg dw (Borrego et al., 2004; Censi et al., 2007; Marmolejo-Rodríguez et al., 2007; Shynu et al., 2011;

Deepulal et al., 2012; Brito et al., 2018; Chi et al., 2021; Costa et al., 2021; de Freitas et al., 2021; Santos et al., 2023) which are close to the values recorded in the present study (85.8 – 225.6 mg/kg dw for the Loire and 20.0 – 97.8 mg/kg dw for the Seine, **Table S5**). Moreover, the values reported in the Loire estuary for these two compartments are consistent with previous studies on REEs in the same studied area, reporting values ranging from 51 to 489 mg/kg dw and from 129.6 to 199.0 mg/kg dw in SPM and sediments, respectively (Thibault de Chanvalon et al., 2016; Lortholarie, 2021).

Total REE concentrations were globally lower in the dissolved phase and higher in SPM or sediments as reported in other studies (Censi et al., 2007; Amyot et al., 2017). These differences indicate that REEs preferentially accumulate in SPM and sediments due to agglomeration processes. Indeed, various studies have shown that REEs tend to coagulate in colloids and aggregate with particulate matter to end up in the sediment at low salinity whereas at high salinity they tend to be solubilized and are mostly distributed in the dissolved phase (Tepe & Bau, 2016; Thibault de Chanvalon et al., 2016). In the present study, the estuarine sites of Loire and Seine (L1 to L8 and S1 to S6) can be associated with low salinities (0.1 to 23.6 g/L, **Table S1**), explaining the higher concentrations in SPM and sediments than in the dissolved phase (**Figure 2**). This phenomenon could also explain the variation in results reported for SPM and sediments between the estuarine and offshore sites in Loire. The salinity of offshore sites (L9 to L13) ranged from 31 to 35 g/L (**Table S1**) and is associated with lower REE concentrations (**Figure 2C, E**). For the dissolved phase, although offshore sites correspond to higher salinities (thus inducing solubilization of REEs), they present similar REE concentrations to estuarine sites (**Figure 2A**). This observation may be due to the global dilution, as well as limited dynamic exchange with particles or sediments offshore compared to within the estuary.

The magnitude of the REE concentrations in SPM and sediments, being slightly higher in the Loire estuary than in the Seine estuary (**Figure 2**), might be explained by the different geogenic compositions of the studied areas (Negrel, 1997), with the Loire presenting a higher natural abundance of REEs or by a possible higher REE contamination in the Loire compared to the Seine.

Inter-site differences could be due to a higher amount of fine particles within the estuary, the MTZ being between L5 and L8 in the Loire and between S5 and S6 in the Seine (**Table S1**). Therefore, grain size and organic matter content were also measured in the sediment samples of both estuaries (**Figure S1**). This allowed to demonstrate that high REE concentrations were rather associated with sediments with low grain size and high OM content, mostly significant for the Loire estuary (**Table S9 and S10**). These data also help to explain the differences in REE concentrations observed between estuarine (L1 to L8) and offshore (L9 to L13) sites. In the Loire, most of estuarine sediments showed lower grain size (D_{50} of 9.1 to 59.5 µm) and higher OM content (6.2 to 15.8 %) than offshore ones, which were mostly sandy (D_{50} from 53.6 to 158.2 µm) and with OM contents from 2.7 to 3.7 % (except in L12, D_{50} grain size = 11.8 µm and OM = 10.3 %) (**Table S5**, **Figure S1A, C**). These results indicate that the REE concentrations in the sediment (**Figure 2**) might also depend on the sediment characteristics, such as grain size and OM. The lower the grain size and the higher the OM content, the higher the REE concentrations. This is also consistent within the Seine estuary where S2 presented a slightly higher grain size (D_{50} of 52.4 *vs* 19.1 ± 10.7 µm in the other sites) and a globally lower OM percentage (1.7 *vs* 7.6 ± 3.7 %) (**Table S5**, **Figure S1B, D**), which therefore results in a lower concentration of REEs in the sediments of that site than in the others (**Figure 2**). Nevertheless, although subtidal sediments showed a lower percentage of OM (9.6 ± 1.6 %) compared to intertidal sediments (15.2 ± 0.6 %) of the same sites (L5, L7 and L8) in Loire (**Table S5**, **Figure S1C**), they did not show lower REE concentrations (**Figure 2**).

To better account for the mineralogical variations of the studied sites and to compare them, REE concentrations in SPM and sediments were normalized to the Al concentrations for each site (**Figure S2**), as Al-normalization is often used for grain-size correction of the concentrations when studying sediments. The differences between the studied sites of the two estuaries were globally eliminated by Al-normalization for both matrices (**Figure 2 and S2**) except in L10 where REE concentrations became higher than in the other sites of Loire (**Figure S2A, C**). The differences between the estuarine (L1 to L8) and offshore (L9 to L13) sites of Loire were also eliminated or reversed with slightly higher REE concentrations in the offshore sites compared to the estuarine sites of Loire (**Figure S2A, C**).

This observation could be due to an underestimation of REE concentrations in the estuarine area using Al-normalization. Indeed, Al is widely used in the wastewater treatment (in coagulation and flocculation processes; Lee et al., 2012) and the Loire estuary might be contaminated by anthropogenic Al, leading to a bias in the Al-normalization results. Therefore, this data treatment might not be appropriated for highly industrialized and contaminated areas, such as the Loire or Seine (Coynel et al., 2016). Al concentrations were actually globally higher in SPM and sediments of estuarine sites (77.7 ± 7.2 and 71.1 ± 11.5 g/kg dw) compared to offshore sites (6.6 ± 6.1 and 20.6 ± 10.0 g/kg dw), confirming the possible bias induced by Al normalization (**Tables S4 and S5**).

4.2. REE distribution

Regarding the REE individual contributions, the distribution of REE classes in the dissolved phase contrasted with those in SPM and sediments of the two estuaries, with a higher contribution of MREEs (mainly due to Gd) and HREEs and a lower LREE contribution than in the two other matrices.

The important HREE contributions in the dissolved phase (**Figure 3A, B**) are consistent with the known REE behavior in the saline water column. Indeed, many studies have highlighted HREE enrichment in seawater (Elderfield & Greaves, 1982; de Baar et al., 1985b; Alibo & Nozaki, 1999; Kulaksiz & Bau, 2007; Piper & Bau, 2013) because LREEs have a higher affinity for SPM while HREEs tend to bind with dissolved ligands (Elderfield & Greaves, 1982; Ma et al., 2019). The offshore sites (L9 to L13) differed from the estuarine sites (L1 to L8) with a higher contribution of HREEs compared to MREEs (**Figure 3A**) which can be explained by the impact of the salinity gradient on REE solubilization in the water column. As explained above, at low salinities, REEs tend to be transferred from the dissolved phase to SPM and sediments, by coagulation which preferentially occurs for LREEs, whereas at high salinities REEs tend to be solubilized in the dissolved phase, preferentially for HREEs (Sholkovitz, 1993; Sholkovitz & Szymczak, 2000; Tepe & Bau, 2016). Combined together, these two phenomena favor an enrichment of HREEs in the dissolved phase that is increasing with the salinity gradient, thus explaining the higher contribution of HREEs in offshore sites.

Concerning SPM and sediments, the higher contribution of LREEs (especially Ce) compared to MREEs and HREEs (**Figure 3C, D, E, F**) is consistent with their known abundance in the Earth's crust where LREEs are globally more abundant than MREEs and HREEs, with Ce being the most abundant REE in the environment (Christie et al., 1998; Bru et al., 2015).

The high contribution of Gd compared to the other REEs in the dissolved phase of both estuaries (**Figure 3**) testifies of a Gd enrichment possibly due to a preferential anthropogenic contamination of this matrix, compared to SPM and sediments. Moreover, the contribution of Gd in the dissolved phase REE patterns from the Seine estuary is higher than that of the Loire estuary (**Figure 3A, B**), suggesting a possible anthropogenic Gd contamination, enhanced in the Seine. Finally, the lower Gd contributions in the dissolved phase REE patterns from the Loire offshore sites (L9 to L13) compared to the estuarine sites (L1 to L8) (**Figure 3A**) highlight a possible anthropogenic contamination of the estuarine area associated with continental releases enhanced by the dilution phenomena occurring offshore.

4.3. Anomalies and estimated Gd anthropogenic inputs

Normalized REE patterns, allowing to consider geogenic background concentrations, highlighted a HREE enrichment, as well as negative Ce anomalies and positive Eu and Gd anomalies, in the dissolved phase of the two estuaries. The HREE enrichment reported in both estuaries (**Figure 4A, B**) is consistent with previous studies highlighting the same phenomenon (Elderfield & Greaves, 1982; de Baar et al., 1985b; Alibo & Nozaki, 1999; Kulaksiz & Bau, 2007; Piper & Bau, 2013), as well as with the behavior of REEs in the water column already discussed (Sholkovitz, 1993; Sholkovitz & Szymczak, 2000; Tepe & Bau, 2016). Similarly, negative Ce anomalies, are often reported, as well as Eu anomalies (Elderfield & Greaves, 1982; Alibo & Nozaki, 1999; Möller et al., 2003, 2021; Piper & Bau, 2013), especially in seawater studies. Indeed, although most of the REEs are redox insensitive and exist in the trivalent form (III) in the environment, Ce and Eu can be oxidized or reduced to Ce (VI) and Eu (II) under specific conditions (de Baar et al., 1985a). The change in oxidation state can impact the solubility of these elements, leading to enrichment or depletion in the dissolved phase of

the water column. In the present study, the negative Ce anomaly (**Figure 4A, B**) indicates of its oxidation to Ce^{4+}, which is less soluble than Ce^{3+}, and tends to coagulate in colloids aggregating to SPM, a typical phenomenon in oxygenated and neutral pH waters (Elderfield & Greaves, 1982; Sholkovitz, 1993; Bau, 1999). Regarding the positive Eu anomaly (**Figure 4A, B**), it should be inherited from water-rock interactions involving Eu^{2+} (more soluble than Eu^{3+}) enriched minerals associated to reducing and/or high-temperature hydrothermal systems (Sverjensky, 1984; Goldstein & Jacobsen, 1988; Danielson et al., 1992). The magnitude differences of the Ce and Eu anomalies between the two estuaries, higher in the Loire than in the Seine, and also higher in the estuarine sites (L1 to L8) than in the offshore sites (L9 to L13) of Loire (**Figure 4A, B and 5A, B**), can therefore be explained by differences in the physicochemical parameters of the studied waters, such as dissolved oxygen, pH, redox (which is known to vary seasonally in the Loire, depending particularly on eutrophication; Minaudo et al., 2015) as well as differences in the geochemical background. Several studies have shown that the magnitude of the Ce anomaly tends to increase with increasing salinity and depth (Elderfield & Greaves, 1982; de Baar et al., 1985b; Sholkovitz, 1993; Möller et al., 2021). The results of the present study show the opposite with higher anomalies in the estuarine sites compared to the offshore sites of Loire (**Figure 4A and 5A**), which are characterized by higher salinity and depth (**Table S1**).

On the contrary to the total REE concentrations, Gd anomalies and anthropogenic Gd concentrations are higher in the Seine than in the Loire, as well as in the estuarine sites (L1 to L8) compared to the offshore sites (L9 to L13) of Loire (**Figure 4A, B, 5C and 6**). These results suggest a greater Gd contamination of the Seine estuary compared to the Loire estuary and of the estuarine area compared to the offshore. They also demonstrate the pressure of industrialization and of the high population density of these estuarine areas, leading to Gd enrichment as shown in many other studies (de Baar et al., 1985b; Alibo & Nozaki, 1999; Elbaz-Poulichet et al., 2002; Kulaksiz & Bau, 2007, 2013; Merschel & Bau, 2015; da Costa et al., 2021; Lortholarie, 2021). The Gd enrichments are often related to its anthropogenic uses (Kümmerer & Helmers, 2000; Rabiet et al., 2009; Verplanck et al., 2010; Hatje et al., 2016; Lerat-Hardy et al., 2019), especially extensive as contrast agents during MRI

(Blomqvist et al., 2022), reaching 22 to 66 tons of Gd used per year (Thomsen, 2017). The difference in Gd contamination between the two estuaries (**Figure 5C and 6**) might be explained by the different population densities, being much higher in the Seine (including the Paris metropolis), and therefore implying higher potential annual releases induced by a likely higher number of MRIs. Moreover, the mean daily water discharges between the two estuaries being much higher during the sampling of the Loire (503 to 807 m^3/s) compared to the Seine (320 to 342 m^3/s) could also be an explanation for the difference of the Gd anomaly magnitudes. The difference between estuarine and offshore areas could be attributed to the distance to the terrestrial sources on the one hand and to the dilution in seawater on the other hand. The estimation of the geogenic and anthropogenic Gd contributions to the total REE concentrations (**Figure 2 and 6**) also allowed to confirm the Gd is mainly due to a natural abundance in the Loire estuary which is the opposite of the Seine estuary, especially under anthropogenic contamination.

A recent study by Rétif et al. (2024) which investigated the REE distribution along the food web of the Loire estuary showed that organisms accumulate REEs. This bioaccumulation was higher in species from lower trophic levels compared to fish belonging to higher trophic levels. However, the highest reported anomalies were found in fish species with Eu, Tb, Gd and Lu anomalies. These results, combined with the present work, indicate a possible transfer of Gd from the dissolved phase to the biota. Additionally, another study on *Anguilla anguilla* from the Loire estuary also highlighted a great accumulation of Gd in the gonads of female organisms (Lortholarie et al., 2021).

Regarding SPM and sediments, the result of normalization, highlighting a HREE depletion (especially in the Loire) associated with no noticeable anomalies (**Figure 4C, D, E, F**), is consistent with the abundance of different REE classes in the Earth's crust but differs from other studies. These studies, including those which focused on the Loire estuary, highlighted a MREE enrichment in SPM and sediments (Thibault de Chanvalon et al., 2016; Lortholarie, 2021; Han et al., 2021, 2023). Nevertheless, the present study, observing anomalies in the dissolved phase, that were absent in SPM or sediments, even though REE concentrations were higher in these two solid matrices, is consistent

with other studies that mostly quantified anomalies in the dissolved phase compared to the particulate phase or sediment (Elbaz-Poulichet et al., 2002; Censi et al., 2007; da Costa et al., 2021).

5. Conclusion

This study comparing the REE levels in the abiotic compartments from the Loire and Seine estuaries highlighted overall higher total concentrations in the Loire than in the Seine, and lower concentrations offshore than within the Loire estuary. These differences could be due either to variations in REE contamination or to differences in the geogenic REE background of both areas, and also imply an anthropogenic contamination of the estuarine area. In both estuaries, total REE concentrations were higher in SPM and sediments than in the dissolved phase which is consistent with the known fate of REEs in aquatic systems. Investigation of individual REE contributions, along with the normalization of REE concentrations by PAAS, highlighted HREE enrichments, as well as Gd enrichments/anomalies in the dissolved phase of both estuaries. On the contrary, the REE distribution patterns in SPM and sediments followed the crustal abundance of the different REE classes for LREEs and MREEs, but highlighted a slight HREE depletion. The high Gd contributions and anomalies measured in the dissolved phase suggest a Gd contamination in the two estuaries, possibly due its extensive anthropogenic use as contrast agent in medicine, as already reported in other estuaries in developed countries. This demonstrates that although REEs tend to accumulate in SPM and sediments, the dissolved phase is the main impacted matrix by anthropogenic uses of REEs. The distribution and normalization results, combined with the estimated anthropogenic Gd concentrations results in the dissolved phase, highlighted that the Gd contamination was higher in the Seine compared to the Loire, rather indicating a high geogenic contribution as an explanation for the high total REE concentrations recorded in the Loire. Finally, higher anthropogenic inputs were reported in the estuarine area compared to the offshore of Loire, confirming the estuarine contamination induced by the important anthropogenic pressures related to their high industrialization and population density. The present work, comparing two major French estuaries with different topographies and pollution levels, provides new data on the distribution of REEs in natural aquatic systems.

Funding and acknowledgment

This project was supported by the Observatory of the Sciences of the Universe Nantes Atlantique (OSUNA, Nantes University, CNRS UAR-3281, UGE, CNAM, univ Angers, IMT Atlantique). The authors thank the French MESRI for the PhD scholarship of J. Rétif. We would also thank the Bio-littoral team as well as A. Baltzer (LETG UMR6554) for the sampling of subtidal sediments and offshore water. Furthermore, we acknowledge S. Bruzac from Ifremer CCEM, L. Chabaud from Pharmacy Faculty of Nantes, A. Kamari from ISOMer and P. Gaudin from LPG for the sample treatment for REE analysis, for the grain size sediment analysis, for the helping hand with sample preparation, for providing technical assistance during the freeze-drying process, respectively. Finally, we thank the interns B. Cai, R. Moncrieffe, M. Olivier and C. Grosgeorge for the help during sampling and sample preparation.

References

Abdelnour, S. A., Abd El-Hack, M. E., Khafaga, A. F., Noreldin, A. E., Arif, M., Chaudhry, M. T., Losacco, C., Abdeen, A., & Abdel-Daim, M. M. (2019). Impacts of rare earth elements on animal health and production: Highlights of cerium and lanthanum. *Science of the Total Environment*, *672*, 1021–1032. https://doi.org/10.1016/j.scitotenv.2019.02.270

Adebayo, S. B., Cui, M., Hong, T., Akintomide, O., Kelly, R. P., & Johannesson, K. H. (2020). Rare earth element cycling and reaction path modeling across the chemocline of the Pettaquamscutt River estuary, Rhode Island. *Geochimica et Cosmochimica Acta*, *284*, 21–42. https://doi.org/10.1016/j.gca.2020.06.001

Alibo, D. S., & Nozaki, Y. (1999). Rare earth elements in seawater: Particle association, shale-normalization, and Ce oxidation. *Geochimica et Cosmochimica Acta*, *63*, 363–372. https://doi.org/https://doi.org/10.1016/S0016-7037(98)00279-8

Amyot, M., Clayden, M. G., Macmillan, G. A., Perron, T., & Arscott-Gauvin, A. (2017). Fate and Trophic Transfer of Rare Earth Elements in Temperate Lake Food Webs. *Environmental Science and Technology*, *51*(11), 6009–6017. https://doi.org/10.1021/acs.est.7b00739

Bau, M. (1999). Scavenging of dissolved yttrium and rare earths by precipitating iron oxyhydroxide: Experimental evidence for Ce oxidation, Y-Ho fractionation, and lanthanide tetrad effect. *Geochimica et Cosmochimica Acta*, *63*(1), 67–77. https://doi.org/https://doi.org/10.1016/S0016-7037(99)00014-9

Blomqvist, L., Nordberg, G. F., Nurchi, V. M., & Aaseth, J. O. (2022). Gadolinium in Medical Imaging - Usefulness, Toxic Reactions and Possible Countermeasures - A Review. *Biomolecules*, *12*(6). https://doi.org/10.3390/biom12060742

Boët, P., Bocquené, G., Bouleau, G., Etchebert, H., Foussard, V., Just, A., Lepage, M., Lobry, J., Moussard, S., & Sirost, O. (2011). *Synthèse du projet BEEST*. https://hal.inrae.fr/hal-02599542

Borrego, J., López-González, N., Carro, B., & Lozano-Soria, O. (2004). Origin of the anomalies in light and middle REE in sediments of an estuary affected by phosphogypsum wastes (south-western Spain). *Marine Pollution Bulletin*, *49*, 1045–1053. https://doi.org/10.1016/j.marpolbul.2004.07.009

Briant, N., Le Monier, P., Bruzac, S., Sireau, T., Araújo, D. F., & Grouhel, A. (2021). Rare Earth Element in Bivalves' Soft Tissues of French Metropolitan Coasts: Spatial and Temporal Distribution. *Archives of Environmental Contamination and Toxicology*, *81*(4), 600–611. https://doi.org/10.1007/s00244-021-00821-7

Brito, P., Prego, R., Mil-Homens, M., Caçador, I., & Caetano, M. (2018). Sources and distribution of yttrium and rare earth elements in surface sediments from Tagus estuary, Portugal. *Science of the Total Environment*, *621*, 317–325. https://doi.org/10.1016/j.scitotenv.2017.11.245

Bru, K., Christmann, P., Labbé, J. F., & Lefebvre, G. (2015). *Panorama 2014 du marché des Terres Rares Rapport public*.

Cánovas, C. R., Basallote, M. D., & Macías, F. (2020). Distribution and availability of rare earth elements and trace elements in the estuarine waters of the Ría of Huelva (SW Spain). *Environmental Pollution*, *267*. https://doi.org/10.1016/j.envpol.2020.115506

Cardon, P. Y., Triffault-Bouchet, G., Caron, A., Rosabal, M., Fortin, C., & Amyot, M. (2019). Toxicity and Subcellular Fractionation of Yttrium in Three Freshwater Organisms: Daphnia magna, Chironomus riparius, and Oncorhynchus mykiss. *ACS Omega*, *4*(9), 13747–13755. https://doi.org/10.1021/acsomega.9b01238

Castor, S. B., & Hedrick, J. B. (2006). Rare Earth Elements. *Industrial Minerals and Rocks*, *7*, 769–792.

Censi, P., Sprovieri, M., Saiano, F., Di Geronimo, S. I., Larocca, D., & Placenti, F. (2007). The behaviour of REEs in Thailand's Mae Klong estuary: Suggestions from the Y/Ho ratios and lanthanide tetrad effects. *Estuarine, Coastal and Shelf Science*, *71*(3–4), 569–579. https://doi.org/10.1016/j.ecss.2006.09.003

Chi, G., Liu, B., Hu, K., Yang, J., & He, B. (2021). Geochemical composition of sediments in the Liao River Estuary and implications for provenance and weathering. *Regional Studies in Marine Science*, *45*, 101833. https://doi.org/10.1016/j.rsma.2021.101833

Christie, T., Brathwaite, B., & Tulloch, A. (1998). Mineral Commodity Report 17 - Rare Earths and Related Elements. *New Zealand Mining*, *24*(7), 1–13.

Chunye, L., Mengchang, H. E., Li, Y., Linsheng, Y., Ruimin, L., & Zhifeng, Y. (2008). Rare earth element content in the SPM of Daliao river system and its comparison with that in the sediments, loess and soils in China. *JOURNAL OF RARE EARTHS*, *26*(3), 414. https://doi.org/https://doi.org/10.1016/S1002-0721(08)60108-8

Costa, L., Mirlean, N., & Johannesson, K. H. (2021). Rare earth elements as tracers of sediment contamination by fertilizer industries in Southern Brazil, Patos Lagoon Estuary. *Applied Geochemistry*, *129*, 104965. https://doi.org/10.1016/j.apgeochem.2021.104965

Coynel, A., Gorse, L., Curti, C., Schafer, J., Grosbois, C., Morelli, G., Ducassou, E., Blanc, G., Maillet, G. M., & Mojtahid, M. (2016). Spatial distribution of trace elements in the surface sediments of a major European estuary (Loire Estuary, France): Source identification and evaluation of anthropogenic contribution. *Journal of Sea Research*, *118*, 77–91. https://doi.org/10.1016/j.seares.2016.08.005

da Costa, A. R. B., Rousseau, T. C. C., Maia, P. D., Amorim, A. M., Sodré, F. F., & Teixeira, C. E. P. (2021). Anthropogenic gadolinium in estuaries and tropical Atlantic coastal waters from Fortaleza, Northeast Brazil. *Applied Geochemistry*, *127*. https://doi.org/10.1016/j.apgeochem.2021.104908

Danielson, A., Möller, P., & Dulski, P. (1992). The europium anomalies in banded iron formations and the thermal history of the oceanic crust. *Chemical Geology*, *97*, 89–100. https://doi.org/https://doi.org/10.1016/0009-2541(92)90137-T

de Baar, H. J. W., Bacon, M. P., Brewer, P. G., & Bruland, K. W. (1985a). Rare earth elements in the Pacific and Atlantic Oceans. *Geochimica et Cosmochimica Acta*, *49*(9), 1943–1959. https://doi.org/10.1016/0016-7037(85)90089-4

de Baar, H. J. W., Brewer, P. G., & Bacon, M. P. (1985b). Anomalies in rare earth distributions in seawater: Gd and Tb*. *Geochimica et Cosmochimica Acta*, *49*, 1961–1969. https://doi.org/https://doi.org/10.1016/0016-7037(85)90090-0

de Freitas, T. O. P., Pedreira, R. M. A., & Hatje, V. (2021). Distribution and fractionation of rare earth elements in sediments and mangrove soil profiles across an estuarine gradient. *Chemosphere*, *264*. https://doi.org/10.1016/j.chemosphere.2020.128431

Deepulal, P. M., Kumar, G., & Sujatha, C. H. (2012). Behaviour of REEs in a tropical estuary and adjacent continental shelf of southwest coast of India: Evidence from anomalies. *Journal of Earth System Science*, *121*(5), 1215–1227.

Elbaz-Poulichet, coise, Seidel, J.-L., & Othoniel, C. (2002). Occurrence of an anthropogenic gadolinium anomaly in river and coastal waters of Southern France. *Water Research*, *36*, 1102–1105. https://doi.org/https://doi.org/10.1016/S0043-1354(01)00370-0

Elderfield, H., & Greaves, M. J. (1982). The rare earth elements in seawater. *Nature*, *296*(5854), 214–219. https://doi.org/10.1038/296214a0

Etcheber, H., Taillez, A., Abril, G., Garnier, J., Servais, P., Moatar, F., & Commarieu, M. V. (2007). Particulate organic carbon in the estuarine turbidity maxima of the Gironde, Loire and Seine estuaries: origin and lability. *Hydrobiologia*, *588*(1), 245–259. https://doi.org/10.1007/s10750-007-0667-9

Freitas, R., Costa, S., D Cardoso, C. E., Morais, T., Moleiro, P., Matias, A. C., Pereira, A. F., Machado, J., Correia, B., Pinheiro, D., Rodrigues, A., Colónia, J., Soares, A. M. V. M., & Pereira, E. (2020). Toxicological effects of the rare earth element neodymium in Mytilus galloprovincialis. *Chemosphere*, *244*. https://doi.org/10.1016/j.chemosphere.2019.125457

Goldstein, S. J., & Jacobsen, S. B. (1988). Rare earth elements in river waters. *Earth and Planetary Science Letters*, *89*, 35–47. https://doi.org/10.1016/0012-821X(88)90031-3

Han, G., Liu, M., Li, X., & Zhang, Q. (2023). Sources and geochemical behaviors of rare earth elements in suspended particulate matter in a wet-dry tropical river. *Environmental Research*, *218*. https://doi.org/10.1016/j.envres.2022.115044

Han, G., Yang, K., & Zeng, J. (2021). Distribution and fractionation of rare earth elements in suspended sediment of the Zhujiang River, Southwest China. *Journal of Soils and Sediments*, *21*, 2981–2993. https://doi.org/10.1007/s11368-021-03008-8

Hatje, V., Bruland, K. W., & Flegal, A. R. (2014). Determination of rare earth elements after pre-concentration using NOBIAS-chelate PA-1®resin: Method development and application in the

San Francisco Bay plume. *Marine Chemistry*, *160*, 34–41. https://doi.org/10.1016/j.marchem.2014.01.006

Hatje, V., Bruland, K. W., & Flegal, A. R. (2016). Increases in Anthropogenic Gadolinium Anomalies and Rare Earth Element Concentrations in San Francisco Bay over a 20 Year Record. *Environmental Science and Technology*, *50*(8), 4159–4168. https://doi.org/10.1021/acs.est.5b04322

Kulaksiz, S., & Bau, M. (2007). Contrasting behaviour of anthropogenic gadolinium and natural rare earth elements in estuaries and the gadolinium input into the North Sea. *Earth and Planetary Science Letters*, *260*, 361–371. https://doi.org/10.1016/j.epsl.2007.06.016

Kulaksiz, S., & Bau, M. (2013). Anthropogenic dissolved and colloid/nanoparticle-bound samarium, lanthanum and gadolinium in the Rhine River and the impending destruction of the natural rare earth element distribution in rivers. *Earth and Planetary Science Letters*, *362*, 43–50. https://doi.org/10.1016/j.epsl.2012.11.033

Kümmerer, K., & Helmers, E. (2000). Hospital effluents as a source of gadolinium in the aquatic environment. *Environmental Science and Technology*, *34*(4), 573–577. https://doi.org/10.1021/es990633h

Laczovics, A., Csige, I., Szabó, S., Tóth, A., Kálmán, F. K., Tóth, I., Fülöp, Z., Berényi, E., & Braun, M. (2023). Relationship between gadolinium-based MRI contrast agent consumption and anthropogenic gadolinium in the influent of a wastewater treatment plant. *Science of the Total Environment*, *877*. https://doi.org/10.1016/j.scitotenv.2023.162844

Lafite, R., & Romana, L.-A. (2001). A Man-Altered Macrotidal Estuary: The Seine Estuary (France): Introduction to the Special Issue. *Estuaires*, *24*, 939.

Lee, K. E., Morad, N., Teng, T. T., & Poh, B. T. (2012). Development, characterization and the application of hybrid materials in coagulation/flocculation of wastewater: A review. *Chemical Engineering Journal*, *203*, 370–386. https://doi.org/10.1016/j.cej.2012.06.109

Lerat-Hardy, A., Coynel, A., Dutruch, L., Pereto, C., Bossy, C., Gil-Diaz, T., Capdeville, M. J., Blanc, G., & Schäfer, J. (2019). Rare Earth Element fluxes over 15 years into a major European Estuary (Garonne-Gironde, SW France): Hospital effluents as a source of increasing gadolinium anomalies. *Science of the Total Environment*, *656*, 409–420. https://doi.org/10.1016/j.scitotenv.2018.11.343

Li, J. X., Zheng, L., Sun, C. J., Jiang, F. H., Yin, X. F., Chen, J. H., Han, B., & Wang, X. R. (2016). Study on Ecological and Chemical Properties of Rare Earth Elements in Tropical Marine Organisms. *Chinese Journal of Analytical Chemistry*, *44*(10), 1539–1546. https://doi.org/10.1016/S1872-2040(16)60963-5

Lortholarie, M., Poirier, L., Kamari, A., Herrenknecht, C., & Zalouk-Vergnoux, A. (2021). Rare earth element organotropism in European eel (Anguilla anguilla). *Science of the Total Environment*, *766*. https://doi.org/10.1016/j.scitotenv.2020.142513

Lortholarie Marjorie. (2021). *Les Terres Rares : Exposition et bioaccumulation de deux espèces clés de l'écosystème estuarien ligérien*. Université de Nantes.

Ma, L., Dang, D. H., Wang, W., Evans, R. D., & Wang, W. X. (2019). Rare earth elements in the Pearl River Delta of China: Potential impacts of the REE industry on water, suspended particles and oysters. *Environmental Pollution*, *244*, 190–201. https://doi.org/10.1016/j.envpol.2018.10.015

Marmolejo-Rodríguez, A. J., Prego, R., Meyer-Willerer, A., Shumilin, E., & Sapozhnikov, D. (2007). Rare earth elements in iron oxy-hydroxide rich sediments from the Marabasco River-Estuary System (pacific coast of Mexico). REE affinity with iron and aluminium. *Journal of Geochemical Exploration*, *94*(1–3), 43–51. https://doi.org/10.1016/j.gexplo.2007.05.003

Merschel, G., & Bau, M. (2015). Rare earth elements in the aragonitic shell of freshwater mussel Corbicula fluminea and the bioavailability of anthropogenic lanthanum, samarium and gadolinium in river water. *Science of the Total Environment*, *533*, 91–101. https://doi.org/10.1016/j.scitotenv.2015.06.042

Minaudo, C., Meybeck, M., Moatar, F., Gassama, N., & Curie, F. (2015). Eutrophication mitigation in rivers: 30 Years of trends in spatial and seasonal patterns of biogeochemistry of the Loire River (1980-2012). *Biogeosciences*, *12*(8), 2549–2563. https://doi.org/10.5194/bg-12-2549-2015

Möller, P., Dulski, P., & De Lucia, M. (2021). Rey patterns and their natural anomalies in waters and brines: The correlation of Gd and Y anomalies. *Hydrology*, *8*(3). https://doi.org/10.3390/hydrology8030116

Möller, P., Morteani, G., & Dulski, P. (2003). Anomalous Gadolinium, Cerium, and Yttrium contents in the Adige and Isarco River waters and in the water of their tributaries (Provinces Trento and Bolzano/Bozen, NE Italy). *Acta Hydrochimica et Hydrobiologica*, *31*(3), 225–239. https://doi.org/10.1002/aheh.200300492

Möller, P., Paces, T., Dulski, P., & Morteani, G. (2002). Anthropogenic Gd in surface water, drainage system, and the water supply of the City of Prague, Czech Republic. *Environmental Science and Technology*, *36*(11), 2387–2394. https://doi.org/10.1021/es010235q

Negrel, P. (1997). Multi-element Chemistry of Loire Estuary Sediments: Anthropogenic vs. Natural Sources. *Estuarine, Coastal and Shelf Science*, *44*, 395–410. https://doi.org/https://doi.org/10.1006/ecss.1996.0139

Ozaki, T., Enomoto, S., Minai, Y., Ambe, S., Ambe, F., & Makide, Y. (2000). Beneficial effect of rare earth elements on the growth of Dryopteris erythrosora. *Journal of Plant Physiology*, *156*(3), 330–334. https://doi.org/10.1016/S0176-1617(00)80070-X

Perrat, E., Parant, M., Py, J. S., Rosin, C., & Cossu-Leguille, C. (2017). Bioaccumulation of gadolinium in freshwater bivalves. *Environmental Science and Pollution Research*, *24*(13), 12405–12415. https://doi.org/10.1007/s11356-017-8869-9

Piper, D. Z., & Bau, M. (2013). Normalized Rare Earth Elements in Water, Sediments, and Wine: Identifying Sources and Environmental Redox Conditions. *American Journal of Analytical Chemistry*, *4*, 69–83.

Pourmand, A., Dauphas, N., & Ireland, T. J. (2012). A novel extraction chromatography and MC-ICP-MS technique for rapid analysis of REE, Sc and Y: Revising CI-chondrite and Post-Archean Australian Shale (PAAS) abundances. *Chemical Geology*, *291*, 38–54. https://doi.org/10.1016/j.chemgeo.2011.08.011

Rabiet, M., Brissaud, F., Seidel, J. L., Pistre, S., & Elbaz-Poulichet, F. (2009). Positive gadolinium anomalies in wastewater treatment plant effluents and aquatic environment in the Hérault watershed (South France). *Chemosphere*, *75*(8), 1057–1064. https://doi.org/10.1016/j.chemosphere.2009.01.036

Rétif, J., Zalouk-Vergnoux, A., Briant, N., & Poirier, L. (2023). From geochemistry to ecotoxicology of rare earth elements in aquatic environments: Diversity and uses of normalization reference

materials and anomaly calculation methods. *Science of the Total Environment*, *856*. https://doi.org/10.1016/j.scitotenv.2022.158890

Rétif, J., Zalouk-Vergnoux, A., Kamari, A., Briant, N., & Poirier, L. (2024). Trophic transfer of rare earth elements in the food web of the Loire estuary (France). *Science of The Total Environment*, *914*. https://doi.org/10.1016/j.scitotenv.2023.169652

Rogowska, J., Olkowska, E., Ratajczyk, W., & Wolska, L. (2018). Gadolinium as a new emerging contaminant of aquatic environments. *Environmental Toxicology and Chemistry*, *37*(6), 1523–1534. https://doi.org/10.1002/etc.4116

Romana, L. A. (1994). Les principaux estuaires français. *Equinoxe: Les Ressources Vivantes de La Mer et l'environnement Littoral*, 38–42.

Santos, A. C. S. S., Souza, L. A., Araujo, T. G., de Rezende, C. E., & Hatje, V. (2023). Fate and Trophic Transfer of Rare Earth Elements in a Tropical Estuarine Food Web. *Environmental Science and Technology*, *57*(6), 2404–2414. https://doi.org/10.1021/acs.est.2c07726

Selleslagh, J., Amara, R., Laffargue, P., Lesourd, S., Lepage, M., & Girardin, M. (2009). Fish composition and assemblage structure in three Eastern English Channel macrotidal estuaries: A comparison with other French estuaries. *Estuarine, Coastal and Shelf Science*, *81*(2), 149–159. https://doi.org/10.1016/j.ecss.2008.10.008

Sholkovitz, E. R. (1993). The geochemistry of rare earth elements in the Amazon River estuary. *Geochimica et Cosmochimica Acta*, *57*(10), 2181–2190. https://doi.org/10.1016/0016-7037(93)90559-F

Sholkovitz, E., & Szymczak, R. (2000). The estuarine chemistry of rare earth elements: comparison of the Amazon, Fly, Sepik and the Gulf of Papua systems. *Earth and Planetary Science Letters*, *179*, 299–309. https://doi.org/https://doi.org/10.1016/S0012-821X(00)00112-6

Shynu, R., Rao, V. P., Kessarkar, P. M., & Rao, T. G. (2011). Rare earth elements in suspended and bottom sediments of the Mandovi estuary, central west coast of India: Influence of mining. *Estuarine, Coastal and Shelf Science*, *94*(4), 355–368. https://doi.org/10.1016/j.ecss.2011.07.013

Sverjensky, D. A. (1984). Europium redox equilibria in aqueous solution. *Earth and Planetary Science Letters*, *67*, 70–78. https://doi.org/https://doi.org/10.1016/0012-821X(84)90039-6

Tepe, N., & Bau, M. (2016). Behavior of rare earth elements and yttrium during simulation of arctic estuarine mixing between glacial-fed river waters and seawater and the impact of inorganic (nano-)particles. *Chemical Geology*, *438*, 134–145. https://doi.org/10.1016/j.chemgeo.2016.06.001

Thibault de Chanvalon, A., Metzger, E., Mouret, A., Knoery, J., Chiffoleau, J. F., & Brach-Papa, C. (2016). Particles transformation in estuaries: Fe, Mn and REE signatures through the Loire Estuary. *Journal of Sea Research*, *118*, 103–112. https://doi.org/10.1016/j.seares.2016.11.004

Thomsen, H. S. (2017). Are the increasing amounts of gadolinium in surface and tap water dangerous? *Acta Radiologica*, *58*(3), 259–263. https://doi.org/10.1177/0284185116666419

Verplanck, P. L., Furlong, E. T., Gray, J. L., Phillips, P. J., Wolf, R. E., & Esposito, K. (2010). Evaluating the behavior of gadolinium and other rare earth elements through large metropolitan sewage treatment plants. *Environmental Science and Technology*, *44*(10), 3876–3882. https://doi.org/10.1021/es903888t

Wang, Z., Yin, L., Xiang, H., Qin, X., & Wang, S. (2019). Accumulation patterns and species-specific characteristics of yttrium and rare earth elements (YREEs) in biological matrices from Maluan

Bay, China: Implications for biomonitoring. *Environmental Research*, *179*. https://doi.org/10.1016/j.envres.2019.108804

Zhou, J., & Fiete, G. A. (2020). Rare earths in a nutshell. *Physics Today*, *73*(1), 66–67. https://doi.org/10.1063/PT.3.4397

Declaration of interests

☒The authors declare that they have no known competing financial interests or personal relationships that could have appeared to influence the work reported in this paper.

☐The authors declare the following financial interests/personal relationships which may be considered as potential competing interests:

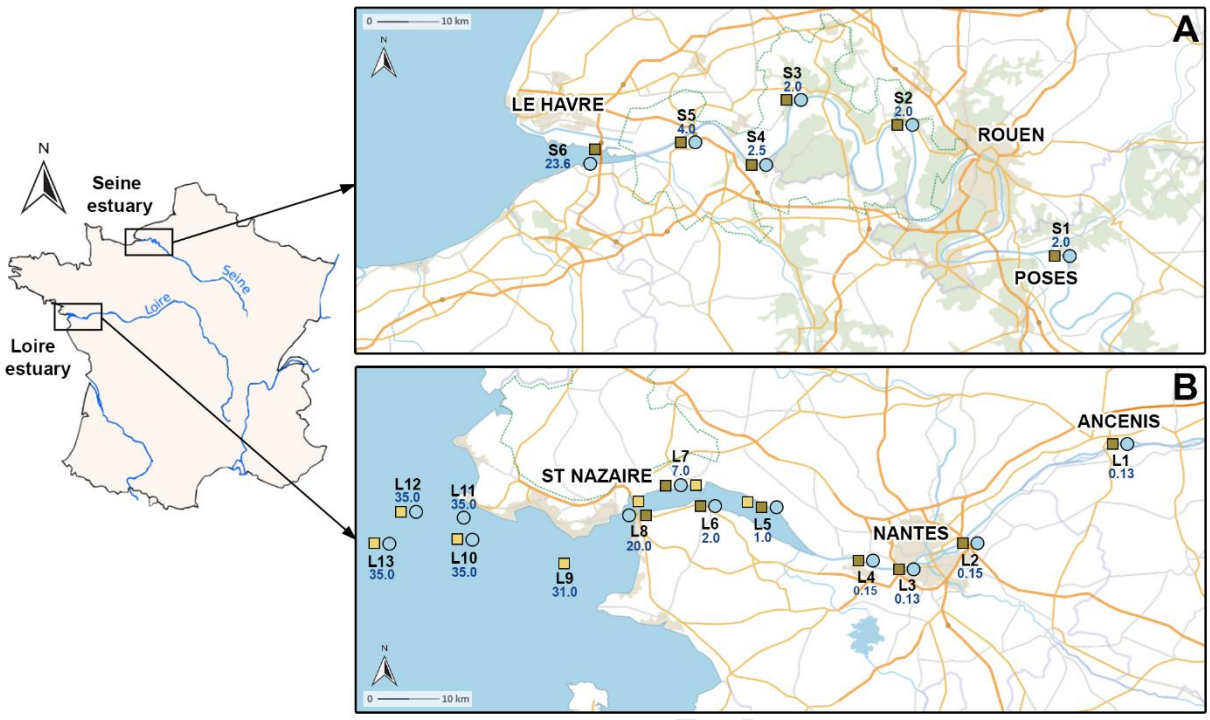

Fig.1. Sampling sites of water (blue circle), intertidal (brown square) and subtidal (yellow square) sediments of the Seine (A) and Loire (B) estuaries with associated salinities (blue font, PSU). S1: Poses, S2: Duclair, S3: Caudebec, S4: Vieux-Port, S5: Tancarville, S6: Baie de Seine, L1: Ancenis, L2: Bellevue, L3: Rezé, L4: Haute-Indre, L5: Cordemais, L6: Paimboeuf, L7: Donges, L8: Mindin, L9: Offshore 1, L10: Offshore 2, L11: Offshore 3, L12: Offshore 4 and L13: Offshore 5.

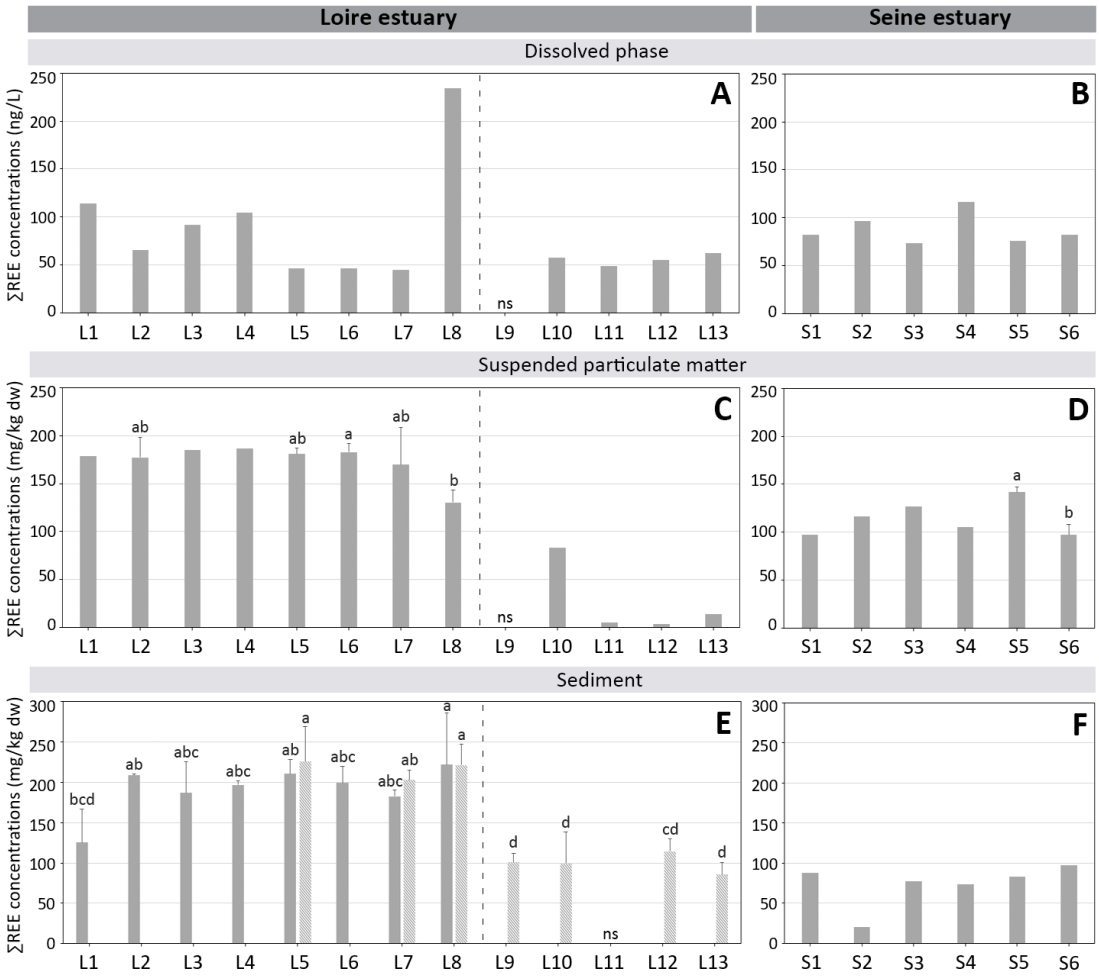

Fig.2. REE concentrations in the dissolved phase (A, B; ng/L), suspended particulate matter (C, D; mg/kg dw) and sediments (E, F; mg/kg dw) of the Loire and Seine estuaries. About sediments: subtidal sediments are presented in hatched histogram bars whereas intertidal sediments are in regular histogram bars. Different letters represent significant differences (ANOVA or t-student test, *p-value* ≤ 0.05) between studied sites for which n > 2, ns: not sampled.

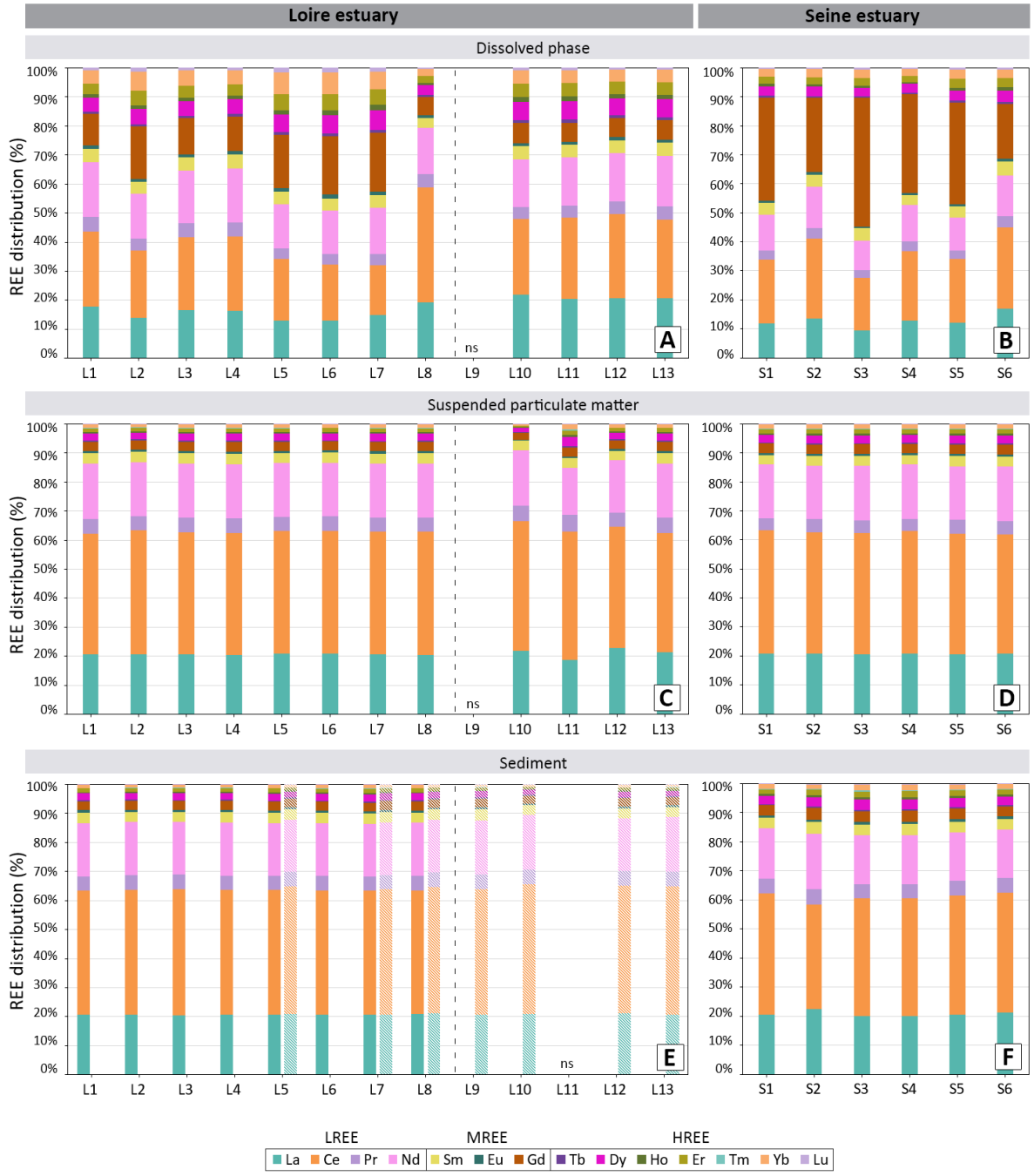

Fig.3. REE distribution (%) in the dissolved phase (A, B), suspended particulate matter (C, D) and sediments (E, F) of the Loire and Seine estuaries. About sediments: subtidal sediments are presented in hatched colors whereas intertidal sediments are in regular colors, ns: not sampled.

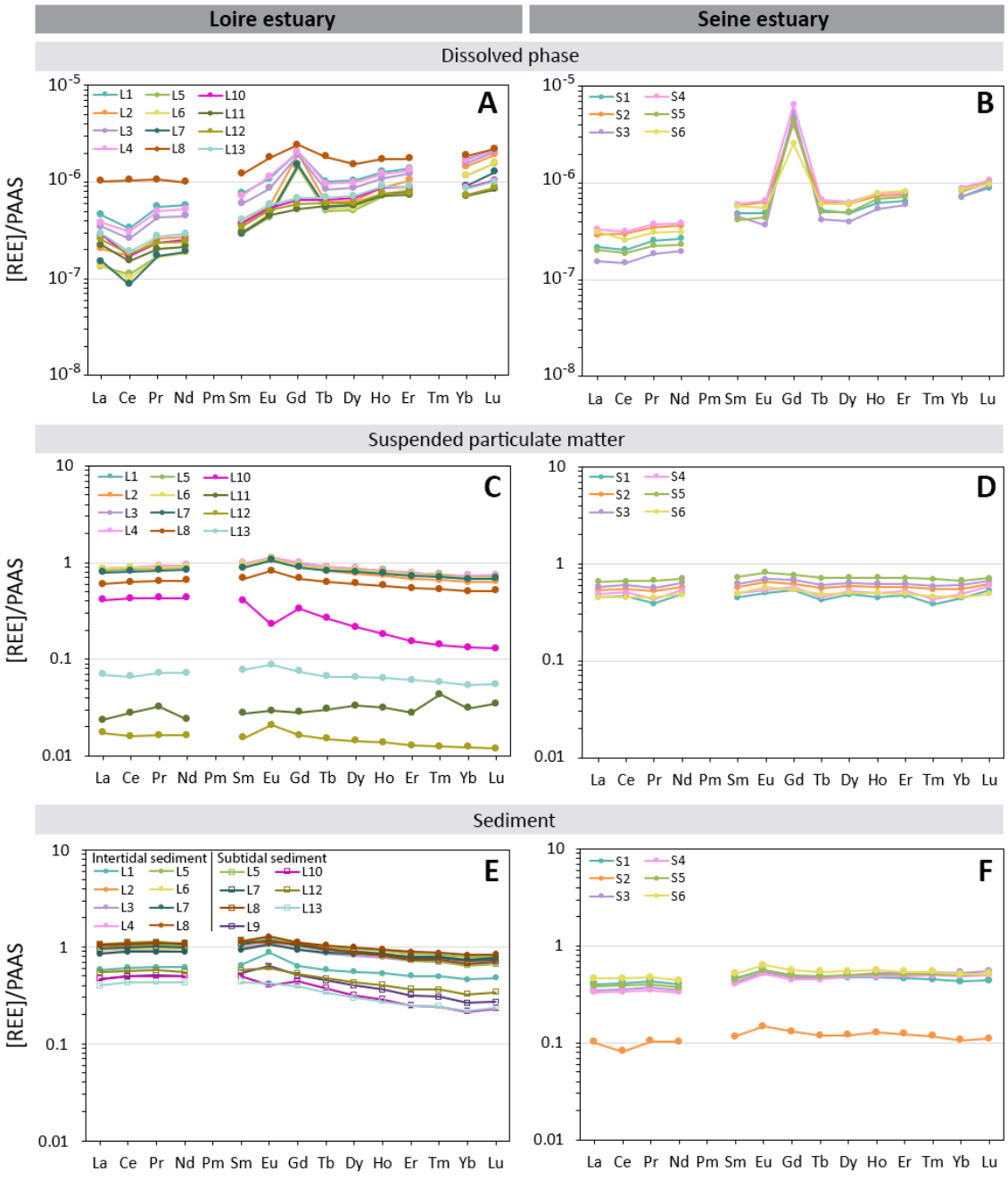

Fig.4. PAAS-normalized REE patterns (log_{10}-scaled axis) for the dissolved phase (A, B), suspended particulate matter (C, D) and sediments (E, F) of the Loire and Seine estuaries. Post-Archean Australian Shale normalization was performed using Pourmand et al. (2012) dataset.

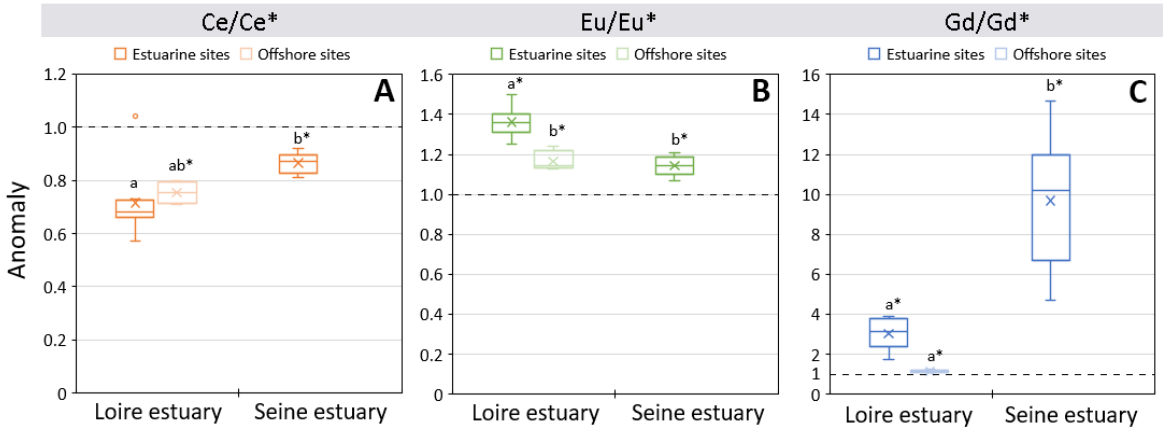

Fig.5. Ce (A), Eu (B) and Gd (C) anomalies in the dissolved phase of the Loire and Seine estuaries. Different letters represent significant differences (Kruskal-Wallis test, *p-value* ≤ 0.05) between studied sites for each element. Values significantly different to 1 (Wilcoxon test, *p-value* ≤ 0.05) are denoted by superscript "*". Lower and upper margins of boxes show 1st and 3rd quartiles, whiskers represent maximum and minimum values, the median is defined by the middle line, the mean by the cross and outliers are drawn as individual points.

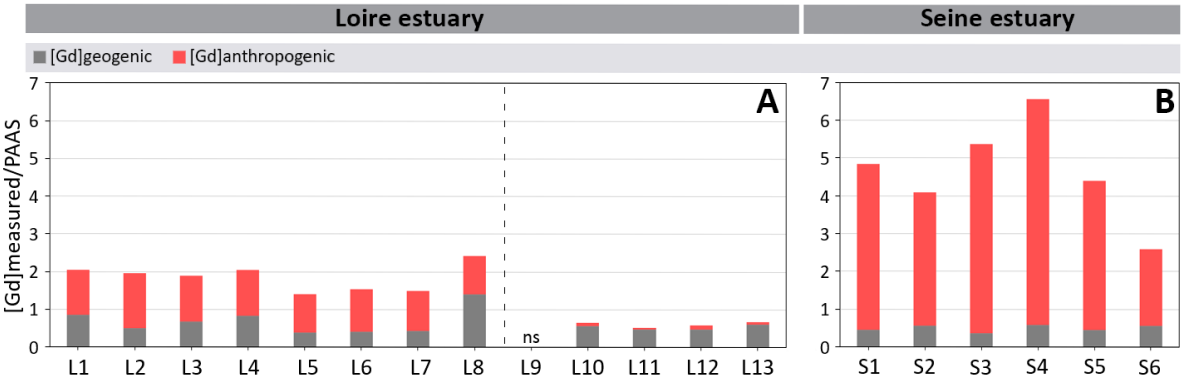

Fig.6. PAAS-normalized Gd concentrations with associated geogenic and anthropogenic concentrations for the dissolved phase of the Loire (A) and Seine (B) estuaries. ns: not sampled.

Table 1. Comparison of total REE concentrations and reported anomalies in the three studied abiotic matrices (dissolved phase, suspended particulate matter (SPM) and sediment) from studies about estuaries of three different continents. Presented data correspond to the minimum and maximum values for each matrix from each study.

Area	Study	Estuary	Total REE concentrations			Anomalies
			Dissolved phase (ng/L)	SPM (mg/kg dw)	Sediment (mg/kg dw)	
America	Marmolejo-Rodríguez et al., 2007	Marabasco (Mexico)			27.5 - 157.3	Eu
	Adebayo et al., 2020	Pettaquamscutt (USA)	253.8 - 2076.9 *			Ce, Eu, Gd
	de Freitas et al., 2021	Jaguaripe (Brazil)			202.0 - 220.0	Ce, Eu
	Costa et al., 2021	Patos Lagoon (Brazil)			75.5 - 253.3	Ce
	Santos et al., 2023	Subaé (Brazil)		102.0 - 163.0	22.6 - 180.0	Eu
Asia	Censi et al., 2007	Mae Klong (Thailand)	2916.2 - 42863.6 *	155.5 - 283.3	14.2 - 127.6	Ce, Eu
	Shynu et al., 2011	Mandovi (India)		83.7 - 202.9	120.4 - 226.5	Ce, Eu
	Deepulal et al., 2012	Cochin (India)			62.0 - 231.0	Ce, Eu
	Chi et al., 2021	Liao (China)			106.6 - 174.7	Eu
Europe	Borrego et al., 2004	Huelva (Spain)			36.0 - 197.7	Ce
	Thibault de Chanvalon et al., 2016	Loire (France)		89.0 - 489.0	195.0 - 199.0	Ce, Eu
	Brito et al., 2018	Tagus (Portugal)			18.0 - 210.0	Ce, Eu
	Lerat-Hardy et al., 2019	Gironde (France)	93.9 - 182.5			Ce, Sm, Gd
	Cánovas et al., 2020	Huelva (Spain)	26.0 - 380.0			Ce, Eu, Gd
	Lortholarie, 2021	Loire (France)	234.0 - 1140.0	51.0 - 333.3	129.6 - 172.0	La, Ce, Gd
	This study	Loire (France)	45.1 - 234.5	3.4 - 186.4	85.8 - 225.6	Ce, Eu, Gd
		Seine (France)	73.1 - 116.3	97.0 - 141.9	20.0 - 97.8	Ce, Eu, Gd

*: values initially presented in nmol/L but converted to ng/L for easier comparison

Graphical abstract